

SORET DRIVEN DOUBLE DIFFUSIVE RAYLEIGH BENARD MARANGONI CONVECTION IN A COMPOSITE LAYER WITH INTERNAL HEAT SOURCE

¹T. Arul Selvamary., ²Shivaraja. J. M., ³Veeranna. Y., ⁴Sumithra. R., ⁵Rashmi. S., ⁶Reshma Raj.,

¹Assistant professor, Department of Mathematics, Jyothi Nivasa College Autonomous affiliated to Bengaluru City University, Bengaluru, Karnataka.

²Assistant professor, Department of Mathematics, Bengaluru North University, Tamaka, Kolar.

^{3&4}Associate professor and professor, Department of UG, PG Studies & Research in Mathematics, Government Science College (Autonomous), Nrupathunga University, Nrupathunga Road, Bengaluru – 560 001, Karnataka.

⁵Rashmi. S and ⁶Reshma Raj, Pg students, Government Science College (Autonomous), Nrupathunga University, Nrupathunga Road, Bengaluru– 560 001, Karnataka.

Abstract

The stability analysis of Soret-driven double diffusive Rayleigh – Benard Marangoni convection in a composite system with an internal heat source is investigated theoretically. The system is confined between lower rigid and upper free horizontal surfaces and adiabatically insulated to temperature and concentration. The system is exposed to uniform and non-uniform salinity gradients. The two-layer model is utilized to govern the momentum equations for fluid and porous layers, which are Navier Stokes and Darcy equations respectively. The graphs are plotted using MATHEMATICA to investigate the influence of solute Rayleigh Number, Soret Number, Darcy number, Thermal Diffusivity Ratio, Thermal Marangoni Number, Solute Marangoni Number, Internal Rayleigh Number, Thermal Depth, Solute Diffusivity Ratio and the ratio of solute to thermal diffusivity on the onset of double-diffusive Rayleigh – Benard Marangoni Convection. Solute Rayleigh number, Soret number, solute diffusivity ratio, and the ratio of solute to thermal diffusivity have a stabilizing impact on the onset of double-diffusive Rayleigh – Benard Marangoni convection.

Keywords: Double Diffusive Convection, Rayleigh – Benard Convection, Marangoni Convection, Soret Effect, Internal Heat Source, and Composite Layer.

1. Introduction

Marangoni convection is convection caused by a surface tension gradient. Even slight changes in temperature or solute concentration can result in convection since surface tension on the free surface is a large function of both those variables. The thermal diffusion process, commonly known as the Soret effect, is induced by a salinity gradient. A horizontal composite layer system of porous and fluid layers with heat and mass transfer taking place through the interface is related to many natural phenomena and various industrial applications. The related problem of a liquid layer overlying a porous layer is also found in many environmental and engineering applications as well. The water layer of a pond or a lake with a muddy bottom layer, transport phenomena that occur from soil to water and vice versa, and the geothermal

system are some of examples of environmental applications. The thermodiffusion effect or the Soret effect is the mass flux in a mixture due to a temperature gradient. This effect is very weak but can be important in the analysis of compositional variation in hydrocarbon reservoirs.

Pearson (1958) investigated the convection cells induced by surface tension. He found that two factors tending to instability would be relevant. The first one is due to temperature variations and the second is due to relative concentration variations. He also found that surface tension forces are responsible for cellular motion in many cases where the criteria given in terms of buoyancy forces would not allow for instability. Nield (1977) first formulated the onset of convection in a fluid layer overlying a porous layer. He proposed an analytic solution including the Marangoni effect at a deformable upper surface. He found that the Marangoni and gravity effects are additive for the onset of convection in a fluid layer overlying a porous medium. Trevisan and Bejan (1985) first reported on a comprehensive numerical study of the natural convection phenomenon occurring inside a porous layer with both heat and mass transfer from the side. Numerical results for overall heat and mass transfer through porous cavity are presented using a Darcy model and compared with scale analysis for several parameters, which governs natural convection. Flinchen et al (1989) investigated the horizontal superposed fluid and the porous layer. The depth ratio, is the ratio of the thickness of the fluid layer to that of the porous layer. The top and bottom walls were kept at different constant temperatures. The onset of convection was detected by a change of slope in the heat flux curve. The results a precipitous decrease in the critical Rayleigh number as the depth of the fluid layer was increased from zero, and an eightfold decrease in the critical wavelength. Anne Silberstein et al (1990) investigated a synthesis of results, both experimental and theoretical, that were obtained from a study of natural convection in fibrous insulating materials presenting a permeable interface to the adjacent fluid layer. Jean.K.Platten (2006) studied the different techniques to measure the Soret coefficient, beam deflection technique, thermal diffusion forced Rayleigh scattering technique, convective coupling and, in particular, the onset of convection in horizontal layers, and the thermogravitational method). Results are provided for several systems, with both negative and positive Soret coefficients, and comparisons between several laboratories are made for the same systems. D.V. Alexandrov et al (2006) analyzed the effect of a temperature-dependent solute diffusion coefficient on the model of unidirectional solidification of a binary melt with a steady-state two-phase zone is studied. The Soret effect (thermodiffusion) is also included in the analysis. The concentration and temperature fields in the liquid, solid, and mixed-state phases are found as functions of all thermophysical parameters. The rate of solidification and two-phase zone thickness are determined as well.

2. Mathematical formulation

We consider a homogeneous porous layer of thickness d_m underlying an incompressible liquid layer of thickness d . Cartesian coordinates are used with origin at the liquid - porous interface. The z direction is opposite to the gravitational acceleration \vec{g} . The bottom of the porous layer is a rigid, and the upper surface of the fluid is free and the system is adiabatically insulated for heat and mass. The temperature difference of fluid layer is $T_0 - T_u$ and of the porous layer is $T_l - T_0$ and that of the total system is $T_l - T_u$. The concentration difference of fluid layer is $C_0 - C_u$, of the porous layer is $C_l - C_0$. And that of the total system is $C_l - C_u$.

Governing Equations

Under the Boussinesq approximation, the equation of continuity, the equation of fluid, the heat equation and the concentration equation and the equation of state are given by,

For fluid layer,

Equation of Continuity,

$$\nabla \cdot \vec{q} = 0 \quad (1)$$

Equation of Momentum,

$$\rho_0 \left[\frac{\partial \vec{q}}{\partial t} + (\vec{q} \cdot \nabla) \vec{q} \right] = -\nabla P + \mu \nabla^2 \vec{q} - \rho g \hat{k} \quad (2)$$

Equation of Energy,

$$\frac{\partial T}{\partial t} + (\vec{q} \cdot \nabla) T = k_T \nabla^2 T + Q \quad (3)$$

Equation of Concentration,

$$\frac{\partial C}{\partial t} + (\vec{q} \cdot \nabla) C = k_C \nabla^2 C + k_T \nabla^2 T \quad (4)$$

Equation of State,

$$\rho = \rho_0 (1 - \alpha_T (T_u - T_0) + \alpha_C (C_u - C_0)) \quad (5)$$

For porous layer,

Equation of Continuity,

$$\nabla_m \cdot \vec{q}_m = 0 \quad (6)$$

Equation of Momentum,

$$\rho_0 \left[\frac{1}{\varphi} \frac{\partial \vec{q}_m}{\partial t} + \frac{1}{\varphi^2} (\vec{q}_m \cdot \nabla_m) \vec{q}_m \right] = -\nabla_m P_m - \frac{\mu}{k} \vec{q}_m - \rho_m g \hat{k} \quad (7)$$

Equation of Energy,

$$\varphi \frac{\partial T_m}{\partial t} + (\vec{q}_m \cdot \nabla_m) T_m = k_{T_m} \nabla_m^2 T_m + Q_m \quad (8)$$

Equation of concentration,

$$\varphi \frac{\partial C_m}{\partial t} + (\vec{q}_m \cdot \nabla_m) C = k_{C_m} \nabla_m^2 C_m + k_{T_m} \nabla_m^2 T_m \quad (9)$$

Equation of State,

$$\rho_m = \rho_0 (1 - \alpha_m (T_l - T_0) + \alpha_m (C_l - C_0)) \quad (10)$$

Basic state solution

The basic state solution of the composite system is obtained for the quiescent flow where velocity, temperature, concentration and pressure are functions of z only and is given by,

For fluid layers,

$$\vec{q}_f = 0, \quad P = P_0(z), \quad T = T_0(z), \quad \rho = \rho_b(z), \quad C = C_b(z)$$

For porous layers,

$$\vec{q}_m = 0, \quad P_m = P_{mb}(z_m), \quad T_m = T_{mb}(z_m), \quad \rho_m = \rho_{mb}(z_m), \\ C_m = C_{mb}(z_m)$$

The temperatures distributions $T_b(z)$ and $T_{mb}(z_m)$ are

$$T_b(z) = -Q \frac{(z^2 - dz)}{2k_T} + \left(\frac{(T_u - T_0)}{d} \right) z + T_0$$

$$T_{mb}(z_m) = \frac{Q_m}{2k_{T_m}} [z_m^2 + d_m z_m] + \left(\frac{(T_0 - T_1)}{d_m} \right) z_m + T_0$$

The concentration distributions $C_b(z)$ and $C_{mb}(z_m)$ are

$$C_b(z) = C_0 + \frac{(C_u - C_0)z}{d}$$

$$C_{mb}(z_m) = C_0 + \frac{(C_0 - C_l)z_m}{d_m}$$

At interface temperature (T_0)

$$T_0 = \left(\frac{T_u k_T d_m + T_l k_{T_m} d}{d d_m} \right) + \left(\frac{d d_m (Q d + Q_m d_m)}{2(d k_{T_m} + k_T d_m)} \right)$$

At interface concentration (C_0)

$$C_0 = \frac{C_u k_C d_m + C_l k_{C_m} d}{k_{C_m} d + k_C d_m}$$

Linear Stability Analysis

Perturbed state

In order to investigate the stability of the basic solution, we superpose perturbations on the system in the form.

for fluid layers,

$$\vec{q} = 0 + \vec{q}', \quad P = P_b(z) + P', \quad T = T_b(z) + \theta, \quad C = C_b(z) + \phi$$

For porous layers,

$$\vec{q}_m = 0 + \vec{q}'_{mb}, \quad P_m = P_{mb}(z_m) + P'_m, \quad T_m = T_{mb}(z_m) + \theta_m, \\ C_m = C_{mb}(z_m) + \phi_m$$

The above equations are substituted in equations (1) to (10) and are linearized in the usual manner. By taking curl twice on equations (2) and (7), the pressure term is eliminated and only the vertical component is retained. The variables are then non-dimensionalized by choosing separate length scales for the two layers so that each layer is of unit depth.

Thus we obtained non-dimensional linearized equations for momentum, temperature, concentration in fluid and porous layers respectively. for fluid layers,

$$(u, v, w) = \frac{k_T}{d}(u^*, v^*, w^*), \quad \theta = (T_0 - T_u)\theta^*, \quad \nabla = \frac{1}{d}\nabla^* \quad (11)$$

$$(x, y, z) = d(x^*, y^*, z^*), \quad \phi = (C_0 - C_u)\phi^*, \quad t = \frac{d^2}{k_T}t^* \quad (12)$$

For porous layers,

$$(u_m, v_m, w_m) = \frac{k_{Tm}}{d_m}(u_m^*, v_m^*, w_m^*), \quad \theta_m = (T_l - T_0)\theta_m^*, \quad \nabla_m = \frac{1}{d_m}\nabla_m^* \quad (13)$$

$$(x_m, y_m, z_m) = d_m(x_m^*, y_m^*, z_m^*), \quad \phi_m = (C_l - C_0)\phi_m^*, \quad t_m = \frac{d_m^2}{k_m}t_m^* \quad (14)$$

Substituting (11) to (14) in the above equations for momentum, temperature, concentration in fluid and porous layers. We obtain the following non-dimensionalised equations.

For fluid layer,

$$\frac{1}{Pr} \frac{\partial(\nabla^2 w)}{\partial t} = \nabla^4 w + \nabla_2^2 \theta Ra_T - \nabla_2^2 \phi Ra_S \quad (15)$$

$$\frac{\partial \theta}{\partial t} - w = \nabla^2 \theta + R_l(2z - 1)w \quad (16)$$

$$\frac{\partial \phi}{\partial t} - w = \tau \nabla^2 \phi + S_r \nabla^2 \theta \quad (17)$$

For porous layer,

$$\frac{Da}{Pr_m} \frac{\partial(\nabla_m^2 w_m)}{\partial t} = -\nabla_m^4 w_m + \nabla_m^2 \theta_m Ra_{T_m} - \nabla_m^2 \phi_m Ra_{S_m} \quad (18)$$

$$A \frac{\partial \theta_m}{\partial t_m} - w_m = \nabla_m^2 \theta_m + R_{I_m} (2z_m - 1) w_m \quad (19)$$

$$\phi \frac{\partial \phi_m}{\partial t_m} - w_m = \tau_m \nabla_m^2 \phi_m + Sr_m \nabla_m^2 \theta_m \quad (20)$$

Where,

$Pr = \frac{\mu}{\rho_0 k_T}$ is the Prandtl number in fluid layer.

$Ra_T = \frac{\rho_0 d^3 g \alpha_T (T_0 - T_u)}{\mu k_T}$ is Rayleigh number in fluid layer.

$Ra_S = \frac{\rho_0 d^3 g \alpha_C (C_0 - C_u)}{\mu k_T}$ is solute Rayleigh number in fluid layer.

$Sr = \frac{\tau(T_0 - T_u)}{(C_0 - C_u)}$ is soret number in fluid layer.

$\tau = \frac{k_C}{k_T}$ is the ratio of solute to temperature diffusivity in fluid layer.

$Pr_m = \frac{\mu \phi}{\rho_0 k_{T_m}}$ is the Prandtl number in porous layer.

$Ra_{T_m} = \frac{\rho_0 d g \alpha'_T (T_l - T_0)}{\mu k_{T_m}}$ is Rayleigh number in porous layer.

$Ra_{S_m} = \frac{k \rho_0 d^3 g \alpha_C (C_l - C_0)}{\mu k_{C_m}}$ is solute Rayleigh number in porous layer.

$Da = \frac{k}{d^2 m}$ is solute Rayleigh number in porous layer.

$Sr_m = \frac{k_{C_m} (T_l - T_0)}{k_{T_m} (C_l - C_0)}$ is soret number in porous layer.

$\tau_m = \frac{k_{C_m}}{k_{T_m}}$ is the ratio of solute to temperature diffusivity in porous layer.

$Ra_{T_m} = \frac{\alpha_T \hat{k}_T^2}{\hat{d}^4} Da Ra_T$ is the Relation between Ra_T and Ra_{T_m}

$Ra_{S_m} = \frac{\alpha_C \hat{k}_C^2}{\hat{d}^4} Da Ra_S$ is the Relation between Ra_S and Ra_{S_m}

Thus the momentum equation in porous layer is transformed in terms of

$Ra_T - Ra_S$.

$$\frac{Da}{Pr} \frac{\partial \nabla^2 w_m}{\partial t} = -\nabla^2 w_m + \frac{\alpha_T \hat{k}_T^2}{\hat{d}^4} Da (\nabla_m^2 \theta_m) Ra_T - \frac{\alpha_C \hat{k}_C^2}{\hat{d}^4} Da (\nabla_m^2 \phi_m) Ra_S$$

The non-dimensionalized equations are subjected to normal mode expansion on the dependent variables in the fluid and porous layers as:

$$\begin{bmatrix} W \\ \theta \\ \phi \end{bmatrix} = \begin{bmatrix} w(z) \\ \theta(z) \\ \phi(z) \end{bmatrix} f(x, y, z) e^{i(lx+my)+nt} \quad (21)$$

$$\begin{bmatrix} W_m \\ \theta_m \\ \phi_m \end{bmatrix} = \begin{bmatrix} w_m(z_m) \\ \theta_m(z_m) \\ \phi_m(z_m) \end{bmatrix} f_m(x_m, y_m, z_m) e^{i(l_mx+m_my)+n_mt} \quad (22)$$

with $\nabla_2^2 f + a^2 f = 0$ and $\nabla_{2m}^2 f_m + a_m^2 f_m = 0$ where a and a_m are the wave numbers, n and n_m are the frequencies, W and W_m are the dimensionless vertical velocities in the fluid and porous layers respectively. As the principle of exchange of stability is valid for the present problem, the time derivatives are dropped, i.e., $n = 0 = n_m$. Where l and m are the horizontal wave number in the x and y directions respectively. Substituting equations (21) and (22) in equations (15) to (20), we get the following ordinary differential equations:

for fluid layer,

$$(D^2 - a^2)w(z) = a^2(Ra_T\theta - Ra_S\phi) \quad (23)$$

$$(D^2 - a^2)\theta(z) + w(z) + (Ra_I(2z - 1)w(z) = 0 \quad (24)$$

$$\tau(D^2 - a^2)\phi(z) + w(z) + Sr(D^2 - a^2)\theta(z) = 0 \quad (25)$$

For porous layer,

$$(D_m^2 - a_m^2)w_m(z_m) = a_m^2(Ra_{T_m}\theta_m - Ra_{S_m}\phi_m) \quad (26)$$

$$(D_m^2 - a_m^2)\theta_m(z_m) + w_m(z_m) + (Ra_{I_m}(2z_m - 1)w_m(z_m) = 0 \quad (27)$$

$$\tau(D_m^2 - a_m^2)\phi_m(z_m) + W_m(z_m) + Sr_m(D_m^2 - a_m^2)\theta_m(z_m) = 0 \quad (28)$$

Where,

a and a_m are the non dimensional horizontal wave number, $\frac{\partial}{\partial z} = D$ and $\frac{\partial}{\partial z_m} = D_m$, Φ and Φ_m are the concentrations θ and θ_m are the temperature in fluid and porous layers respectively. W and W_m are dimensionless vertical velocity distribution in fluid and porous layers respectively.

3. Boundary Conditions

Boundary conditions at the fluid and porous layer interface have a great effect on the prediction of convection stability in a composite layer. The interface effect also determines the flow pattern, temperature mass distributions and heat transfer rates. Equations (23) to (28) are to be solved subjected to the following appropriate velocity, temperature and concentration boundary conditions.

The velocity boundary conditions are:

At the free surface of the fluid layer,

$$W(1) = 0$$

$$D^2W(1) + Ma_T a^2 \theta(1) + Ma_S a^2 \phi(1) = 0$$

At the rigid surface of the porous layer,

$$W_m(0) = 0$$

At interface,

$$W(0) = \frac{\hat{d}}{\hat{k}_T} W_m(1)$$

$$D^2W(0) = \frac{\hat{d}^3}{\hat{k}_T} D_m^2 W_m(1)$$

$$D^3W(0) = \frac{\hat{d}^4}{\hat{k}_T D\alpha} D_m W_m(1)$$

Adiabatic temperature boundary condition:

At the top of the fluid layer,

$$D\theta(1) = 0$$

At the bottom of the porous layer,

$$D_m \theta_m(0) = 0$$

At interface,

$$\theta(0) = \frac{\hat{k}_T}{\hat{d}} \theta_m(1)$$

$$D\theta(0) = D_m \theta_m(1)$$

Adiabatic concentration boundary condition:

At the top of the fluid layer

$$D\Phi(1) = 0$$

At the bottom of the porous layer

$$D_m \Phi_m(0) = 0$$

At interface

$$\Phi(0) = \frac{\hat{k}_C}{\hat{d}} \Phi_m(1)$$

$$D\Phi(0) = D_m \Phi_m(1)$$

The system comprising of equations (23) to (24) corresponds to the fluid medium and the system comprising of equations (25) to (28) corresponds to the porous medium along with the boundary conditions forms an eigenvalue problem with Ra_T being the eigenvalue. Since both systems consist of space varying coefficients. It is no longer possible to obtain a closed form solution of the problem. We therefore use a regular perturbation method to solve the eigenvalue problem.

4. Method of solution by Regular Perturbation Technique

An eigen value problem with Ra_T as an eigen value that has to be solved for different salinity gradients. The horizontal wavenumber a is negligibly small. Hence, the eigen value problem is solved by regular Perturbation technique with wave number a as a perturbation parameter accordingly, the variables W , Φ and θ expanded in powers of a^2 as,

$$(w(z), \theta(z), \phi(z)) = \sum_{i=0}^{\infty} (a^2)^i (W_i(z), \theta_i(z), \Phi_i(z)) \quad (29)$$

$$(w_m(z_m), \theta_m(z_m), \phi_m(z_m)) = \sum_{i=0}^{\infty} (a_m^2)^i (W_{mi}(z_m), \theta_{mi}(z_m), \Phi_{mi}(z_m)) \quad (30)$$

Substituting equation (29) and (30) into equation (23) to (28) yields a sequence of equation for the unknown functions.

$W_i(z), W_{mi}(z_m), \theta_i(z), \theta_{mi}(z_m), \Phi_i(z), \Phi_{mi}(z_m)$ for $i = 0, 1, 2, 3 \dots$

The zeroth order equations are:

$$D^4 W_0(z) = 0$$

$$D_m^2 W_{m0}(z_m) = 0$$

$$D^2 \theta_0(z) = 0$$

$$D_m^2 \theta_{m0}(z_m) = 0$$

$$D^2 \Phi_0(z) = 0$$

$$D_m^2 \Phi_{m0}(z_m) = 0$$

The corresponding velocity boundary conditions of zeroth order are:

$$W_0(1) = 0$$

$$D^2 W_0(1) = 0$$

$$W_{m0}(0) = 0$$

$$W_0(0) = \frac{\hat{d}}{\hat{k}_T} W_{m0}(1)$$

$$D^2 W_0(0) = \frac{\hat{d}^3}{\hat{k}_T} D_m^2 W_{m0}(1)$$

$$D^3 W_0(0) = -\frac{\hat{d}^4}{\hat{k}_T} D_m W_{m0}(1)$$

The corresponding adiabatic thermal boundary conditions of zeroth order are:

$$D \theta_0(1) = 0$$

$$D_m \theta_{m0}(1) = 0$$

$$\theta_0(0) = \frac{\hat{k}_T}{\hat{d}} \theta_{m0}(1)$$

$$D\theta_0(0) = D_m \theta_{m0}(0)$$

The corresponding adiabatic concentration boundary conditions of zeroth order are:

$$D\Phi_0(1) = 0$$

$$D_m \Phi_{m0}(0) = 0$$

$$\Phi_0(0) = \frac{\hat{k}_C}{\hat{d}} \Phi_{m0}(1)$$

$$D\Phi_0(0) = D_m \Phi_{m0}(1)$$

The solutions to zeroth order equations are:

$$W_0(z) = 0$$

$$W_{m0}(z_m) = 0$$

$$\theta_0(z) = \hat{T}$$

$$\theta_{m0}(z_m) = 1$$

$$\Phi_0(z) = \hat{C}$$

$$\Phi_{m0}(z_m) = 1$$

The equations of first order of a^2 are:

$$D^4 W_1(z) = Ra_T \hat{T} - Ra_S \hat{C} \quad (31)$$

$$D_m^4 W_{m1}(z_m) = -Ra_{Tm} + Ra_{Sm} \quad (32)$$

$$D^2 \theta_1(z) + W_1(z) + R_l(2z - 1)W_1(z) = \hat{T} \quad (33)$$

$$D_m^2 \theta_{m1}(z_m) + W_{m1}(z_m) + R_{lm}(2z_m + 1)W_{m1}(z_m) = 1 \quad (34)$$

$$\tau D^2 \Phi_1(z) + W_1(z) + Sr D^2 \theta_1(z) = \tau \hat{C} + Sr \hat{T} \quad (35)$$

$$\tau_m D_m^2 \Phi_{m1}(z_m) + W_{m1}(z_m) + Sr_m D_m^2 \theta_{m1}(z_m) = 1 \quad (36)$$

The corresponding velocity boundary conditions of first order of a^2 are:

$$W_1(1) = 0$$

$$D^2 W_1(1) + Ma_T \hat{T} + Ma_S \hat{C} = 0$$

$$W_{m1}(0) = 0$$

$$W_1(0) = \frac{1}{\hat{k}_T \hat{d}} W_m(1)$$

$$D^2 W_1(0) = \frac{\hat{d}}{\hat{k}_T} D_m^2 W_m(1)$$

$$D^3W_1(0) = -\frac{\hat{d}^2}{Da\hat{k}_T}D_mW_m(1)$$

The solutions to equations (31) and (32) after applying velocity boundary conditions , we obtain,

$$W_1(z) = \left(A_8 + A_{10}z + A_2z^2 + A_4z^3 + \frac{\hat{T}}{24}z^4 \right) Ra_T + \left(\left(A_7 + A_9z + A_1z^2 + A_3z^3 - \frac{\hat{C}}{24}z^4 \right) Ra_S \right) + \left(\frac{1}{\hat{d}\hat{k}_T Da} + A_{12}z - \frac{\hat{T}}{6}z^3 \right) Ma_T + \left(\frac{\hat{C}}{\hat{d}\hat{k}_T\hat{T}Da} + A_{11}z - \frac{\hat{C}}{6}z^3 \right) Ma_S$$

$$W_m(z_m) = \left(A_6z_m - \frac{\hat{T}^2 Da}{2}z_m^2 \right) Ra_T + \left(A_5z_m + \frac{\hat{C}^2 Da}{2}z_m^2 \right) Ra_S + \left(\frac{1}{Da}z_m \right) Ma_T + \left(\frac{\hat{C}}{\hat{T}Da}z_m \right) Ma_S$$

Where,

$$A_1 = \frac{\hat{k}_C^2 Da}{2\hat{k}_T \hat{d}^3}, \quad A_2 = -\frac{\hat{k}_T Da}{2 \hat{d}^3}, \quad A_3 = -\left(\frac{\hat{k}_C}{12\hat{d}} + \frac{A_1}{3} \right), \quad A_4 = -\left(\frac{\hat{k}_T}{12\hat{d}} - \frac{A_2}{3} \right)$$

$$A_5 = -\left(\frac{6\hat{k}_T Da A_3}{\hat{d}^2} - \frac{\hat{k}_C^2 Da}{\hat{d}^4} \right), \quad A_6 = -\left(\frac{\hat{k}_T^2 Da}{\hat{d}^4} - \frac{6\hat{k}_T Da A_4}{\hat{d}^2} \right),$$

$$A_7 = -\left(\frac{A_5}{\hat{d}\hat{k}_T} + \frac{\hat{k}_C^2 Da}{2\hat{k}_T \hat{d}^5} \right), \quad A_8 = \left(\frac{A_6}{\hat{d}\hat{k}_T} - \frac{\hat{k}_T Da}{2\hat{d}^5} \right),$$

$$A_9 = -A_7 - A_1 - A_3 + \frac{\hat{k}_C}{12\hat{d}}, \quad A_{10} = -A_8 - A_2 - A_4 - \frac{\hat{k}_T}{24\hat{d}}$$

5. Compatibility condition

Compatibility condition is obtained by integrating the temperature and the concentration equations. Integrating temperature and concentrations equations (33) and (34) between $z=0$ and $z=1$, and multiplying equation (35) and (36) by $\frac{1}{\hat{d}^2}$ and integrate between $z_m = 0$ and $z_m = 1$ and adding the resulting equations, we obtain the compatibility condition as,

$$\left\{ \begin{array}{l} \frac{Sr}{\tau} (1 - R_I) \int_0^1 W_1 f(z) dz + \frac{2R_I Sr}{\tau} (1 - R_I) \int_0^1 z W_1 f(z) dz \\ + \frac{Sr_m (1 + R_{Im})}{\tau_m \hat{d}^2} \int_0^1 W_{m1} f_m(z_m) dz_m + \frac{2R_{Im} Sr_m}{\tau_m \hat{d}^2} \int_0^1 z_m W_{m1} f_m(z_m) dz_m \\ - \frac{1}{\tau} \int_0^1 W_1 g(z) dz - \frac{1}{\tau_m \hat{d}^2} \int_0^1 W_{m1} g_m(z_m) dz_m \end{array} \right\} = -\frac{\hat{k}_C}{\hat{d}} - \frac{1}{\hat{d}^2}$$

By substituting the expression for W_1 and W_{m1} and $f(z) = f_m(z_m) = 1$ into the above equation, integrating and solving we obtain critical Rayleigh number Rc_1 .

$$Rc_1 = \frac{\Sigma - \Pi_1 Ra_S - \Pi_2 Ma_T - \Pi_3 Ma_S}{\Pi_4}$$

Where,

$$\Pi_1 = (B2 + B6 + B10 + B14 + B18 + B22),$$

$$\Pi_2 = (B3 + B7 + B11 + B15 + B19 + B23),$$

$$\Pi_3 = (B4 + B8 + B12 + B16 + B20 + B23),$$

$$\Pi_4 = (B1 + B5 + B9 + B13 + B17 + B21)$$

$$B_1 = \frac{Sr}{\tau} (1 - R_I) \left(\frac{A_{10}}{2} + \frac{A_2}{3} + \frac{A_4}{4} + A_8 + \frac{\hat{k}_T}{120 d} \right);$$

$$B_2 = \frac{Sr}{\tau} (1 - R_I) \left(\frac{A_9}{2} + \frac{A_1}{3} + \frac{A_3}{4} + A_7 - \frac{\hat{k}_C}{120 d} \right);$$

$$B_3 = -\frac{(-1 + R_I) Sr}{24 d^2 \tau} (12 + d k_T); \quad B_4 = -\frac{(-1 + R_I) Sr k_C}{8 d^2 \tau k_T} (-12 + d k_T);$$

$$B_5 = \frac{R_I Sr}{\tau} \left(\frac{2A_{10}}{3} + \frac{A_2}{2} + \frac{2A_4}{5} + A_8 + \frac{\hat{k}_T}{72 d} \right);$$

$$B_6 = -\frac{R_I Sr}{\tau} \left(\frac{2A_9}{3} + \frac{A_1}{2} + \frac{2A_3}{5} + A_7 - \frac{\hat{k}_C}{72 d} \right); \quad B_7 = \frac{R_I Sr}{3 d^2 \tau} + \frac{2 k_T R_I Sr}{45 d \tau};$$

$$B_8 = \frac{5 K_C R_I Sr}{3 d^2 k_T \tau} - \frac{8 k_C R_I Sr}{45 d \tau}; \quad B_9 = \frac{(1 + R_{Im}) Sr_m (3 A_6 d^4 - D a k_T^2)}{6 d^6 \tau_m}$$

$$B_{10} = \frac{(1 + R_{Im}) Sr_m (3 A_5 d^4 - D a k_C^2)}{6 d^6 \tau_m}; \quad B_{11} = \frac{k_T Sr_m}{2 d^3 \tau_m} + \frac{k_T R_{Im} Sr_m}{2 d^3 \tau_m};$$

$$B_{12} = \frac{k_C Sr_m}{2 d^3 \tau_m} + \frac{k_C R_{Im} Sr_m}{2 d^3 \tau_m}; \quad B_{13} = \frac{2 A_6 R_{Im} Sr_m}{3 d^2 \tau_m} - \frac{D a k_T^2 R_{Im} Sr_m}{4 d^6 \tau_m};$$

$$B_{14} = \frac{2 A_5 R_{Im} Sr_m}{3 d^2 \tau_m} - \frac{D a k_C^2 R_{Im} Sr_m}{4 d^6 \tau_m}; \quad B_{15} = \frac{2 k_T R_{Im} Sr_m}{3 d^3 \tau_m};$$

$$B_{16} = \frac{2 k_C R_{Im} Sr_m}{3 d^3 \tau_m}; \quad B_{17} = -\frac{1}{\tau} \left(\frac{A_{10}}{2} + \frac{A_2}{3} + \frac{A_4}{4} + A_8 + \frac{\hat{k}_T}{120 d} \right);$$

$$\begin{aligned}
 B_{18} &= -\frac{1}{\tau} \left(\frac{A_9}{2} + \frac{A_1}{3} + \frac{A_3}{4} + A_7 - \frac{\hat{k}_c}{120d} \right); & B_{19} &= -\frac{1}{2d^2\tau} - \frac{k_T}{24d\tau}; \\
 B_{20} &= -\frac{k_c}{8d\tau} - \frac{3k_c}{2d^2k_T\tau}; & B_{21} &= -\frac{A_6}{2d^2\tau_m} + \frac{Dak_T^2}{6d^6\tau_m}; \\
 B_{22} &= -\frac{A_5}{2d^2\tau_m} + \frac{Dak_c^2}{6d^6\tau_m}; & B_{23} &= -\frac{k_T}{2d^3\tau_m}; & B_{24} &= -\frac{k_c}{2d^3\tau_m}
 \end{aligned}$$

6. Graphical Interpretations

The onset of Rayleigh-Bénard-Marangoni convection in a composite layer is investigated, with a focus on the critical conditions for the onset of instability. The study examines how the Rayleigh number varies with the depth ratio, incorporating the effects of key parameters such as the solute Rayleigh number, Soret number, Darcy number, thermal Marangoni number, solute Marangoni number, internal Rayleigh number, thermal diffusivity ratio, solute diffusivity ratio, and the ratio of solute to thermal diffusivity. The stability analysis is performed using linear stability theory, and the critical Rayleigh number is determined as a function of the governing parameters. The results, presented graphically, reveal the combined effects of thermal and solutal buoyancy, interfacial tension gradients, and the porous medium properties on the stability thresholds. Specific trends are observed, such as the destabilizing influence of the thermal and solutal Marangoni numbers and the stabilizing role of the Darcy number, which characterizes the permeability of the porous medium. Parameters like the Soret number and diffusivity ratios significantly impact the coupling between thermal and solutal fields, influencing the onset of convection. For clarity, certain parameters are held constant during the analysis, and their values are chosen based on physical relevance to the problem. This comprehensive investigation provides insights into the fundamental mechanisms driving convection in composite systems. The fixed value of the parameters are $D_a = 0.03$, $M_{aT} = 5$, $M_{as} = 5$, $R_l = 0.1$, $S_r = 0.5$, $R_{as} = 100$, $\hat{\kappa}_T = 1.0$, $\hat{\kappa}_c = 1.0$ and $\tau = 0.3$.

Figure-1 illustrates the impact of the various values Darcy number $D_a = 0.03, 0.04$ and 0.05 on thermal convection in a porous medium, particularly focusing on the onset convection. For a fixed depth ratio, it is evident that as Da increases, flow resistance decreases, as reflected by the reduction in the critical Rayleigh number. This reduction highlights that a higher Da destabilizes the system, allowing convective motion to commence at lower Rayleigh numbers and thereby promoting the earlier onset of DDRBM convection. The physical interpretation of this phenomenon is tied to the permeability of the medium. As Da increases, the porous medium becomes more permeable, reducing the damping effect of viscous forces on flow and enhancing the convective instability. Consequently, the system transitions from a more stable to a less stable state as Da rises. Additionally, the convergence of curves at both ends of the plot suggests consistent system behavior at extreme values of Da . The porous medium exhibits behavior similar to free fluid convection. These trends confirm that Da is a critical parameter governing the stability and onset of convection in porous systems.

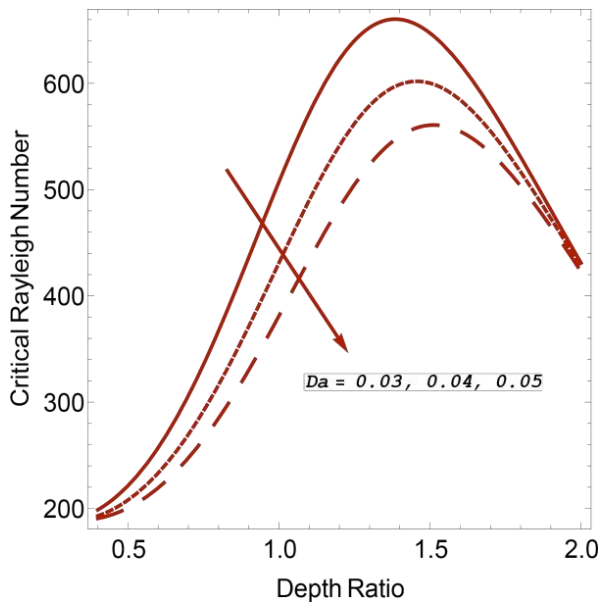


Figure-1: The effect of Darcy number (D_a) on critical Rayleigh number (Ra_C)

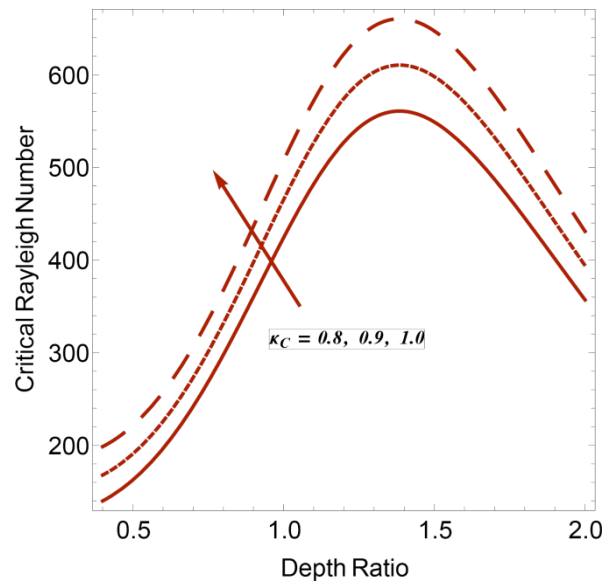


Figure-2: The effect of Solute diffusivity (κ_C) on critical Rayleigh number (Ra_C)

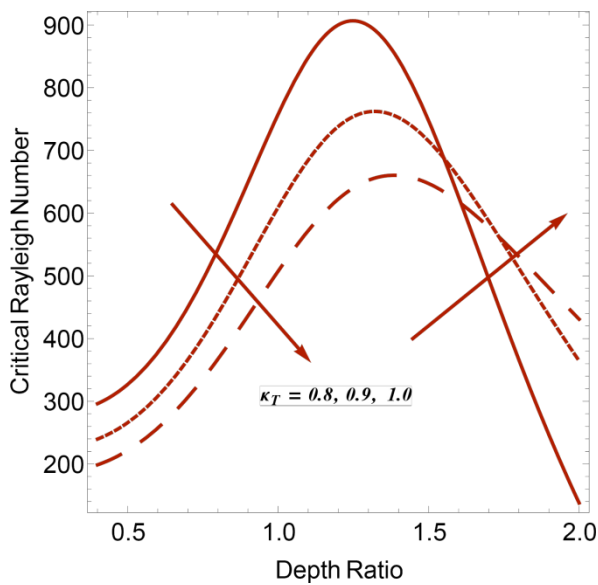


Figure-3: The effect of Thermal diffusivity (κ_T) on critical Rayleigh number (Ra_C)

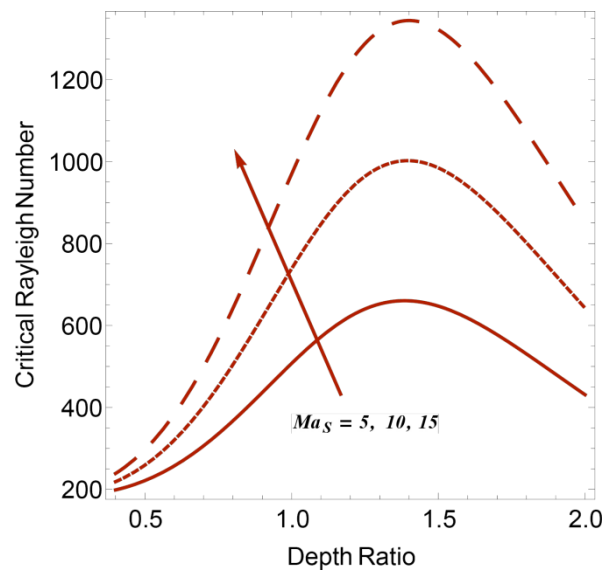


Figure-4: The effect of Solutal Marangoni number (Ma_{as}) on critical Rayleigh number (Ra_C)

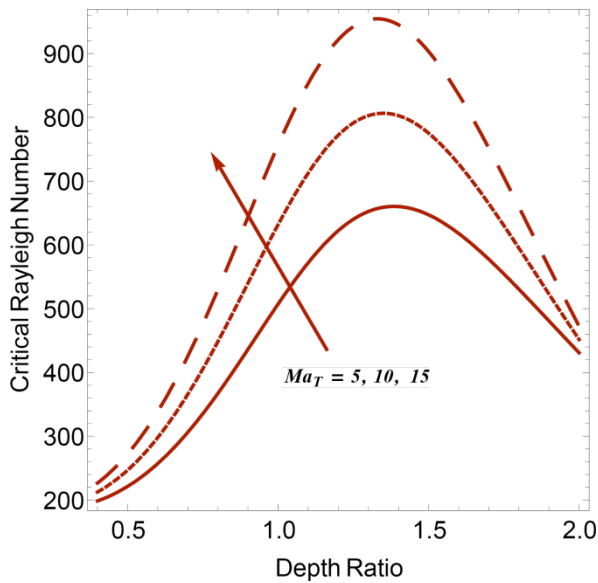


Figure-5: The effect of Solutal Marangoni number (Ma_T) on critical Rayleigh number (R_{ac})

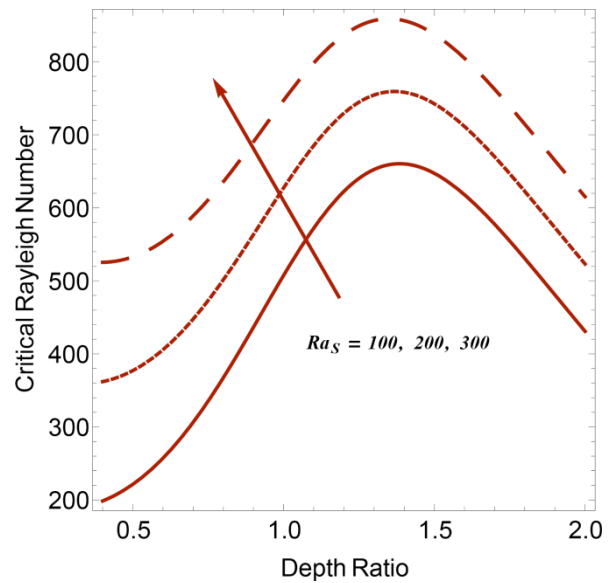


Figure-6: The effect of Solutal Rayleigh number (R_{as}) on critical Rayleigh number (R_{ac})

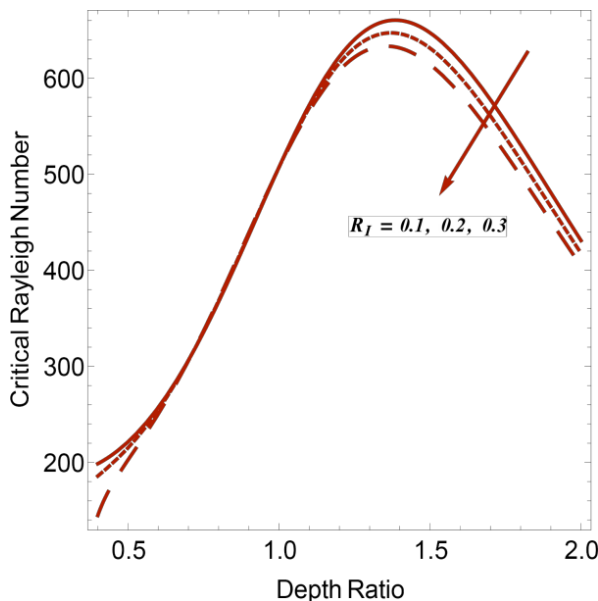


Figure-7: The effect of Internal Rayleigh number (R_I) on critical Rayleigh number (R_{ac})

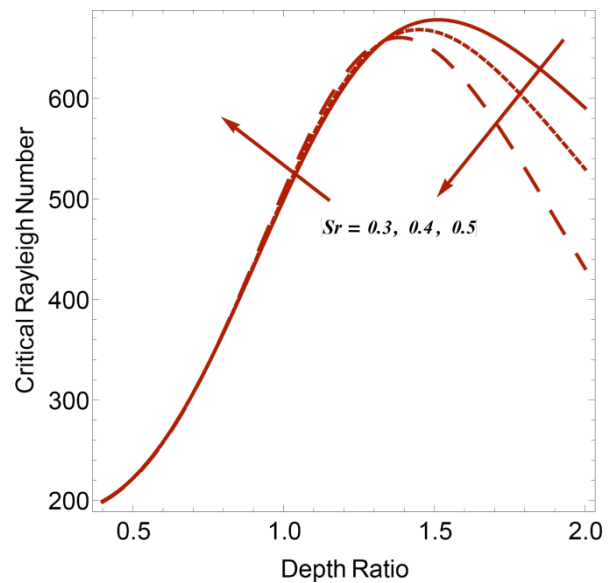


Figure-8: The effect of Soret number (Sr) on critical Rayleigh number (R_{ac})

Figure-2 illustrates the influence of the solute diffusivity ($\kappa_c = 0.8, 0.9$ and 1) on DDRBM convection in a composite layer. For a fixed value of the depth ratio, an increase in the Rayleigh number indicates that flow resistance increases with higher values of the diffusivity ratio. Consequently, this parameter tends to stabilize the system, thereby delaying the onset of DDRBM convection. But the effect different values of thermal diffusivity ($\kappa_T = 0.8, 0.9$ and 1) plays opposite role as shown in figure-3 and plays dual

role. Figures 4 and 5 illustrate the influence of Solutal and Thermal Marangoni numbers ($M_{as} = M_{aT} = 5, 10 \text{ and } 15$) on DDRBM convection. As the Rayleigh number increases, the flow resistance intensifies due to enhanced buoyancy effects. This resistance becomes more pronounced for higher values of the Solutal and Thermal Marangoni numbers (M_{as} and M_{aT}), indicating that interfacial tension gradients play a significant role in stabilizing the flow. Consequently, DDRBM convection can be delayed or suppressed under conditions with sufficiently large Marangoni numbers. This suggests that the interplay between thermal and solutal effects provides a mechanism to regulate convection in the system, potentially extending the stability regime for certain parameter ranges. Such findings are critical for understanding and optimizing transport processes in systems governed by coupled thermal and solutal effects. Figure- 6 illustrates that an increase in the Solutal Rayleigh number ($R_{as} = 100, 200 \text{ and } 300$) leads to a corresponding rise in the overall Rayleigh number (R_a). This increase in (R_{as}) enhances the concentration gradients within the fluid, which delays the onset of convection by increasing the stabilizing effect of solutal buoyancy forces. Consequently, a higher (R_{as}) stabilizes the onset of Double Diffusive Rayleigh-Bénard Marangoni (DDRBM) convection. Figure-7 demonstrates that an increase in the Internal Rayleigh number ($R_I = 0.1, 0.2 \text{ and } 0.3$) enhances the internal heat generation within the fluid. This additional heat source reduces the thermal stability of the system, thereby hastening the onset of convection. As a result, an increase in (R_I) destabilizes the system, leading to the earlier onset of Double Diffusive Rayleigh-Bénard Marangoni (DDRBM) convection. These results underscore the destabilizing role of internal heat sources in systems influenced by coupled thermal and solutal effects, providing insights into the thermal management and stability of such configurations. Figure -8 demonstrates that an increase in the Soret parameter ($S_r = 0.3, 0.4 \text{ and } 0.5$) leads to an increase in the critical Rayleigh number R_{ac} across all salinity gradients. This rise in (S_r) enhances the thermal diffusivity within the system, which accelerates the onset of convection by reducing the thermal resistance. Consequently, the increase in (S_r) destabilizes the system, the onset of Rayleigh-Bénard Marangoni convection at lower stability thresholds. These findings emphasize the destabilizing influence of thermal stratification in systems where both thermal and solutal gradients govern the fluid behavior.

7. Conclusion

Double Diffusive Rayleigh-Barnard-Marangoni (DDRBM) convection in a composite layered system, incorporating the Soret effect and a constant heat source, is analyzed and solved in closed form using the Regular Perturbation method. This study investigates the interplay between thermal and solutal buoyancy forces, surface tension gradients, and the Soret-driven mass diffusion on the stability and dynamics of the system.

The following conclusions are drawn:

1. Effect of increasing the values of ratio of solute to thermal diffusivity ,solute diffusivity and solute Rayleigh number increase the critical Rayleigh number. Consequently, it stabilizes the onset of double diffusive Rayleigh Benard Marangoni convection with constant heat source.
2. Effect of increasing the values of solute Marangoni number and thermal Marangoni number increases the critical Rayleigh number. Consequently, it stabilizes the onset of double diffusivity Rayleigh Benard Marangoni convection with constant heat source.

3. Effect of increasing the values of solet number decreases critical Rayleigh number. Consequently, it destabilizes the onset of double diffusive Rayleigh Benard Marangoni convection with constant heat source.
4. Effect of increasing the values of internal Rayleigh number decreases critical Rayleigh number. Consequently, it destabilizes the onset of double diffusive Rayleigh Benard Marangoni convection with constant heat source.

8. Reference:

- 1] R. A. Pearson, "On convection cells induced by surface tension", 1958.
- 2] D. A. Nield, "Onset of convection in a Fluid Layer Overlying a Layer of porous Medium", J Fluid Mech. 81 ,1977, 513-522
- 3] F. Chen and C. F Chen, "Experimental investigation of convective stability in a superposed fluid and porous layer when heated from below", J Fluid Mech. vol. 207, pp. 311- 321, 1989.
- 4] A. Silberstein, C. Langlais, and E. Arquis, "Natural Convection in Light Fibrous Insulating Materials with Permeable Interfaces: Onset Criteria and Its Effect on the Thermal Performances of the Product", Journal of Thermalinsulation, vol. 14, pp. 22-42, July, 1990.
- 5] M. Z. Saghir, P. Mahendran and M. Hennenberg, "Marangoni and Gravity Driven Convection in a Liquid Layer Overlying a Porous Layer: Lateral and Bottom Heating Conditions", Energy Sources, vol. 27, pp. 151-171, 2005.
- 6] J. K. Platten, "The Soret effect: review of recent experimental results", J of Applied Mechanics, val. 73, pp. 5-15, 2006.
- 7] D. V. Alexandrov, and D. L. Aseev, "Directional solidification with a two-phase zone: thermodiffusion and temperature-dependent diffusivity", Computational Materials Science, val. 37, pp. 1-6, 2006.
- 8] Tsai, R., and J. S. Huang. "Numerical study of Soret and Dufour effects on heat and mass transfer from natural convection flow over a vertical porous medium with variable wall heat fluxes." Computational Materials Science 47, no. 1, 23-30, 2009.
- 9] Sarma, G. Sreedhar, Ra K. Prasad, and K. Govardhan. "The combined effect of chemical reaction, thermal radiation on steady free convection and mass transfer flow in a porous medium considering Soret and Dufour effects." IOSR Journal of Mathematics 8, no. 2, 67-87, 2013.
- 10] Srinivasacharya, D., and O. Surender. "Non-Darcy mixed convection in a doubly stratified porous medium with Soret-Dufour effects." International Journal of Engineering Mathematics, 2014.
- 11] Reddy, D. Srinivas, and K. Govardhan. "Effect of viscous dissipation, Soret and Dufour effect on free convection heat and mass transfer from vertical surface in a porous medium." Procedia Materials Science 10: 563-571, 2015.
- 12] Sarma, G. Sreedhar, and K. Govardhan. "Thermo-diffusion and Diffusionthermo effects on free convective heat and mass transfer from vertical surface in a porous medium with viscous dissipation in the presence of Thermal radiation." Archives of Current Research International 3, no. 1, 1-11, 2016.
- 13] Sumithra R., Komala B., and Manjunatha, N. , "The onset of Darcy–Brinkman– convection in a composite system with thermal diffusion", Heat Transfer, 51(1), pp. 604-620, 2022.
- 14] Izzati Khalidah ,Nor Fadzillah Mohd Mokhtar, Zarina Bibi Ibrahim, "Control Effect on Rayleigh-Benard Convection in Rotating Nanofluids Layer with DoubleDiffusive Coefficients", CFD letters, vol 14 pp.3, 2022.
- 15] Sumithra R., Komala B., "Onset of triple diffusive thermosolutal convection in a composite system", Heat Transfer, pp.2974-2994, 2023.